



Effect of welding parameters on mechanical and microstructural properties of AA6082 joints produced by friction stir welding

P. Cavaliere^{a,*}, A. Squillace^b, F. Panella^a

^a Department of “Ingegneria dell’Innovazione”, Engineering Faculty, University of Salento, Via per Arnesano, I-73100 Lecce, Italy

^b Department of Materials and Production Engineering, Engineering Faculty, University of Naples “Federico II”, I-80125 Naples, Italy

ARTICLE INFO

Article history:

Received 21 September 2006

Received in revised form 3 July 2007

Accepted 10 September 2007

Keywords:

Friction stir welding

Processing parameters

Fatigue

ABSTRACT

The effect of processing parameters on mechanical and microstructural properties of AA6082 joints produced by friction stir welding was analysed in the present study. Different welded specimens were produced by employing a fixed rotating speeds of 1600 rpm and by varying welding speeds from 40 to 460 mm/min. The joints mechanical properties were evaluated by means of tensile tests at room temperature. In addition, fatigue tests were performed by using a resonant electro-mechanical testing machine under constant amplitude control up to 250 Hz sinusoidal loading. The fatigue tests were conducted in axial control mode with $R = \sigma_{\min}/\sigma_{\max} = 0.1$, for all the welding and rotating speeds used in the present study. The microstructural evolution of the material was analysed according to the welding parameters by optical observations of the jointed cross-sections and SEM observations of the fractured surfaces were done to characterize the weld performances.

© 2007 Elsevier B.V. All rights reserved.

1. Introduction

The friction stir welding (FSW) technology is being targeted by modern aerospace industry for high performance structural applications (Mishra and Ma, 2005). If compared to traditional welding techniques, FSW strongly reduces the presence of distortions and residual stresses (Bussu and Irving, 2003; John et al., 2003; Jata et al., 2000). FSW technology requires a thorough understanding of the process and the evaluation of consequent welds mechanical properties are needed in order to use the FSW process for production of components in aerospace applications. For this reason, detailed research and qualification work is required (Lockwood et al., 2002). Based

on friction heating at the facing surfaces of two sheets to be joined, in the FSW process a special tool with a properly designed rotating probe travels down the length of contacting metal plates, producing an highly plastically deformed zone through the associated stirring action. The localized thermo-mechanical affected zone is produced by friction between the tool shoulder and the plate top surface, as well as plastic deformation of the material in contact with the tool (Guerra et al., 2003). The probe is typically slightly shorter than the thickness of the work piece and its diameter is typically slight larger than the thickness of the work piece (Ulysse, 2002). The microstructure evolution and the resulting mechanical properties depend strongly on the variation of

* Corresponding author. Tel.: +39 0832297357; fax: +39 0832325004.

E-mail address: pasquale.cavaliere@unile.it (P. Cavaliere).

0924-0136/\$ – see front matter © 2007 Elsevier B.V. All rights reserved.

doi:10.1016/j.jmatprotec.2007.09.050

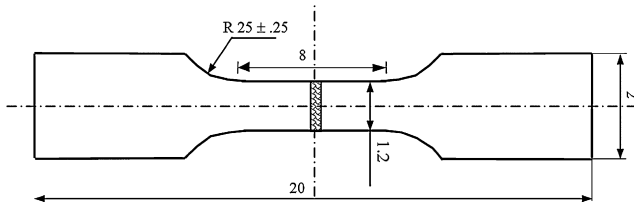


Fig. 1 – Specimens geometry used in the present study.

the processing parameters leading to a wide range of possible performances (Cavaliere et al., 2006). The FSW process is a solid-state process and therefore solidification structure is absent in the weld and the problem related to the presence of brittle inter-dendritic and eutectic phases is eliminated (Cavaliere et al., 2006). Some aluminium alloys can be resistance welded with an extensive surface preparation due to oxide formation. On the other hand, FSW can be used to join most Al alloys as the surface oxide is not a deterrent for the process and therefore no particular cleaning operation is needed prior to welding. In FSW the work piece does not reach the melting point and the mechanical properties of the welded zone (especially when attention is focused on heat-treatable light alloys) are much higher compared to those provided by traditional techniques. In fact, the undesirable low mechanical properties microstructure resulting from melting and re-solidification is absent in FSW welds leading to improved mechanical properties, such as ductility and strength in some alloys (Rhodes et al., 1997; Sato et al., 2003; Berbon et al., 2001). In this way, the welds are characterized by low distortion, lower residual stresses and absence of micro-defects and then of retained products dimensional stability.

Fatigue is the principal cause of failure for welded joints in mechanical components; the application of FSW technology is in particular dependence on mechanical performances, which are strongly affected by the processing parameters, as James et al. (2005) showed the different fatigue behaviour of two Al–Mg alloys as a function of welding speed. In addition, Ericsson and Sandstrom (2003) showed the variation of fatigue life of AA6082 joints with the welding speed, comparing the results with conventional fusion welding techniques. Al–Mg

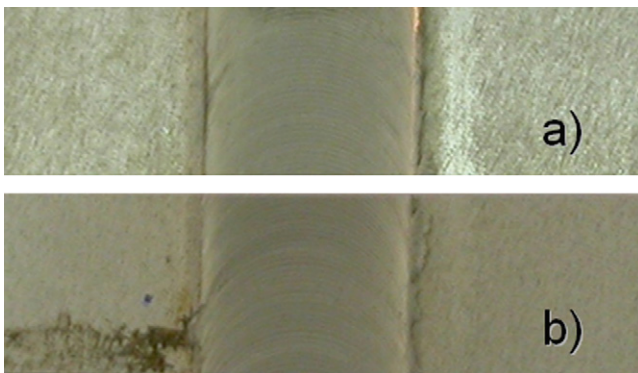


Fig. 2 – Macroscopic aspect of the welds obtained by employing an advancing speed of 115 mm/min (a) and 325 mm/min (b).

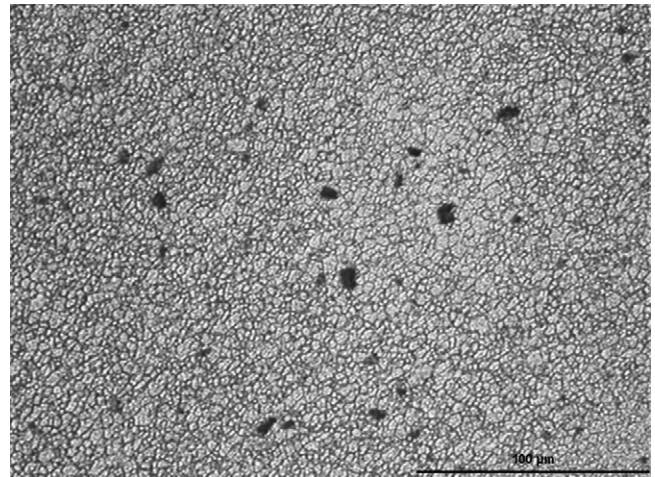


Fig. 3 – Microstructure of the nugget zone of the specimen welded at 115 mm/min.

and Al–Mg–Si alloys plates of different thickness, joined with different welding speeds, have been studied also by Dickerson and Przydatek (2003).

The present work is aimed to the evaluation of the welding speed effect on mechanical and microstructural behaviour of AA6082 welded plates with thickness 4 mm, obtained by different FSW applications.

2. Experimental procedure

The material under investigation was a 6082 commercial aluminium alloy produced by Pechiney under the form of rolled sheets of 4 mm thickness. Two hundred millimetres length \times 80 mm rectangular plates were welded perpendicularly to the rolling direction, after standard T6 heat treatment. Such thermal treatment results in a considerable improvement of the material corrosion resistance. The employed rotating velocities of the cylindrical threaded tool was



Fig. 4 – Initial microstructure of the studied alloy revealing the classical elongated grains belonging to the rolling operations.

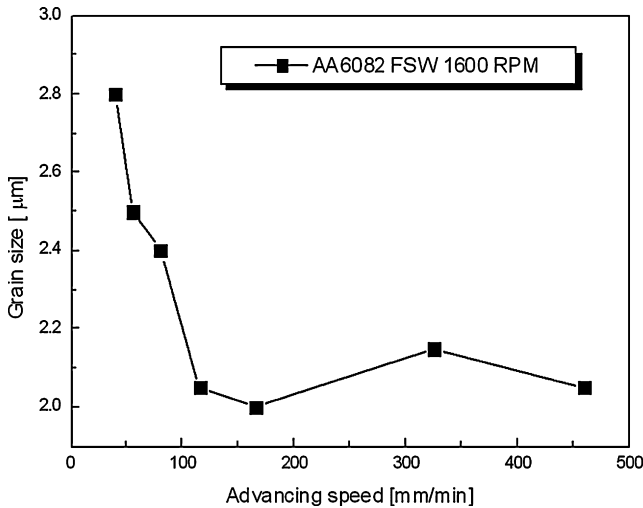


Fig. 5 – Measured mean grain size as a function of welding speed.

1600 rpm while the advancing selected speeds were 40, 56, 80, 115, 165, 325 and 460 mm/min. The pin of the tool had a diameter of 6.0 mm and was 3.9 mm long. A 14 mm diameter shoulder was used and the tilt angle was set equal to 3°.

The machine used for the production of the joints was instrumented with a Kistler three-channel load cell in order to record both forces along the tool axis, hereon denoted as FZ, and along the welding direction, hereon denoted as FX, for all the produced welds. Acquisition scan rate changed as a function of the processing parameters in order to record two time samples per tool revolution, in all the examined conditions. In addition, some sheets were instrumented with thermocouples, perpendicularly to the welding direction, in order to monitor the temperature profiles as a function of the distance from the weld line.

Some specimens for the microstructural analyses were prepared by standard metallographic techniques and etched with Keller's reagent to reveal the grain structure. A statistical analysis was performed in the nugget based on light microscopy images performing the measurements on 300 grains for each condition. Tensile tests were performed in order to evaluate the mechanical properties of the joints obtained in the different welding conditions. The tensile tests were carried out at room temperature using a MTS 810 testing machine with initial strain rate of 10^{-3} s^{-1} . Specimens were sectioned in the perpendicular direction along the weld line by employing an electrical discharge machine (EDM), the dimensions are shown in Fig. 1. Endurance fatigue tests were performed by a resonant electro-mechanical testing machine under constant loading control up to 250 Hz sine wave loading (TESTRONIC™ $50 \pm 25 \text{ kN}$, produced by RUMUL, SUI) in both low and high regimes. The cyclic fatigue tests were conducted under axial total stress amplitude control mode under fully reversed, push-pull, tension loading ($R = \sigma_{\min}/\sigma_{\max} = 0.1$). All the mechanical tests were performed up to failure. A FEGSEM (JEOL-JSM 6500 F) was used to study the fracture surfaces of the material after tensile and fatigue tests.

3. Results and discussion

3.1. Friction stir welding studies

FSW has become a very effective tool in solving the joining problems of profiled sheets with material continuity, without using different joining methods; particularly in case of aerospace industry, where high ductility and tensile strength are required. In the present work, different FSW butt welds of AA6082 sheets were successfully obtained by varying the processing parameters; no macroscopic defects were observed on the surfaces (Fig. 2) and the welded joints were mechanically and metallurgically characterized.

3.2. Microstructural behaviour

The microstructural behaviour of 6082 aluminium alloy joined by friction stir welding was studied by employing optical

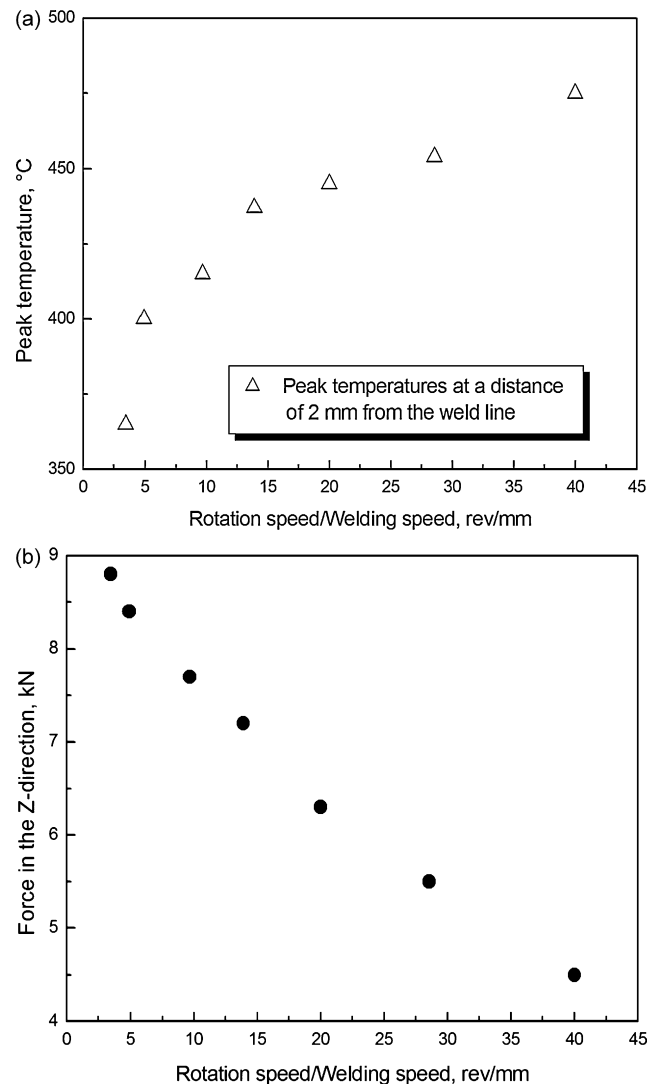


Fig. 6 – Variations of peak temperatures (a) (reached at a distance of 2 mm from the weld line) and the regime forces in the Z-direction (b) as a function of the revolutionary pitch for all the studied joints.

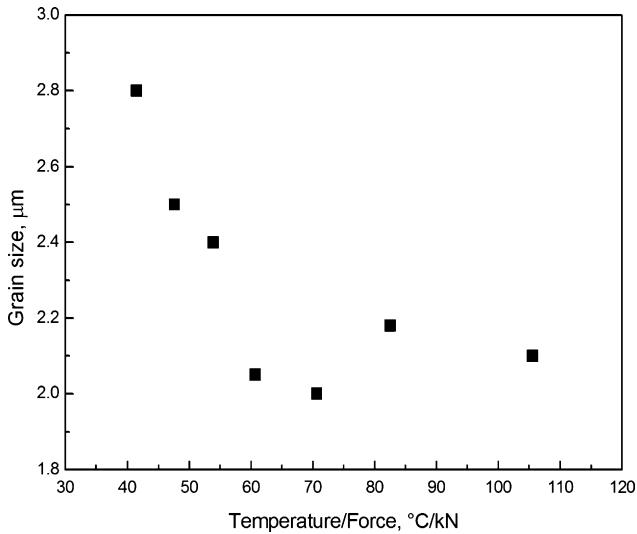


Fig. 7 – Coupling effect of force and temperature to the measured grain size in the nugget zone.

microscopy in all the conditions of welding speed at the chosen rotating one. In all the welding conditions, the flow of material inside the nugget is evidence of substantial plastic stirring during FSW. In Fig. 3 the micrographs of the centre of the nugget zones of a sample (in cross-sections) joined by employing a welding speed of 115 mm/min are shown. The microstructure of the material appears as very fine and equiaxed grains in all the welding conditions as can be noted by the difference with the starting microstructure revealing the classical elongated grains belonging to the rolling operations (Fig. 4). A strong difference in grain size and distribution was observed for different ranges of travel speed; up to 115 mm/min the microstructure appears recrystallized but not so uniform because of the different temperature and true strain reached during deformation at lower speeds. By increasing the travel speed the nugget microstructure appears more

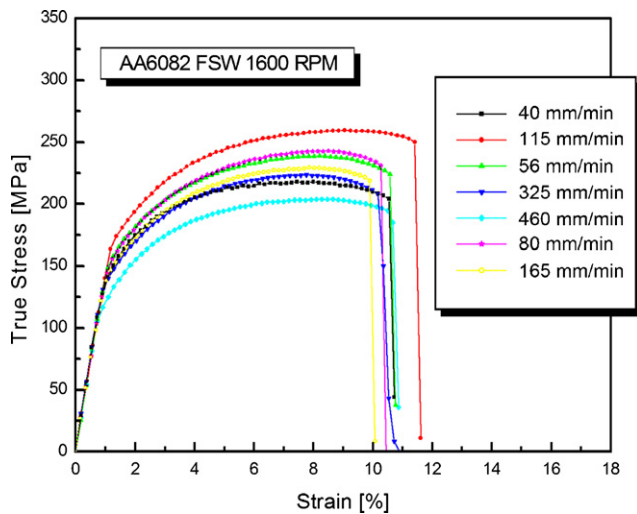


Fig. 8 – Tensile properties of the studied joints revealing the variation of the welds strength by varying the welding speed.

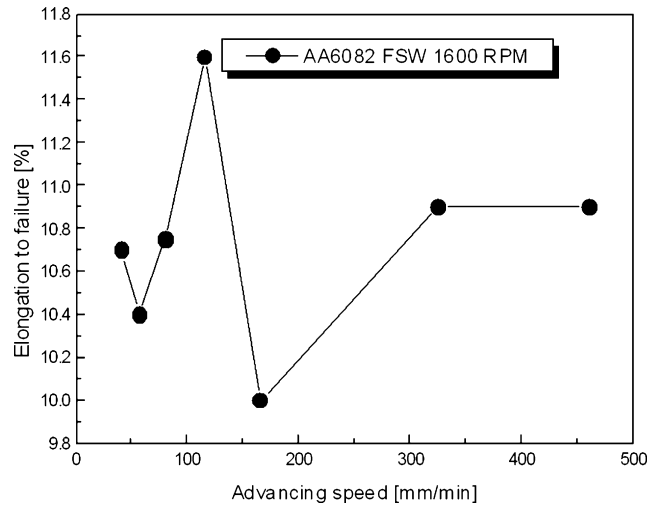


Fig. 9 – Elongation to failure as a function of welding speed.

fine and uniform. By increasing the travel speed it seems that the combination between hot working and dynamic recovery and recrystallization is optimal for the chosen conditions. The mean area of the grains was measured by using an image analyser on 300 grains for each condition, a strong variation in the mean grain size was observed by increasing the advancing speed from 40 to 165 mm/min up to a plateau corresponding to no further variations by increasing the speed up to 460 mm/min (Fig. 5). This is typical of aluminium alloys in which the nugget mean grain size decrease with increasing travel speed, at a given rotation speed, up to a minimum and after it starts to increase again (Hassan et al., 2003). For this alloy, in the studied conditions, it seems that the optimal ratio between rotational and travel speed is 14.

In Fig. 6 they are plotted the variations of peak temperatures (reached at a distance of 2 mm from the weld line) and the regime forces in the Z-direction as a function of the revolutionary pitch for all the studied joints. It can be noted as the temperature increases in a parabolic way while

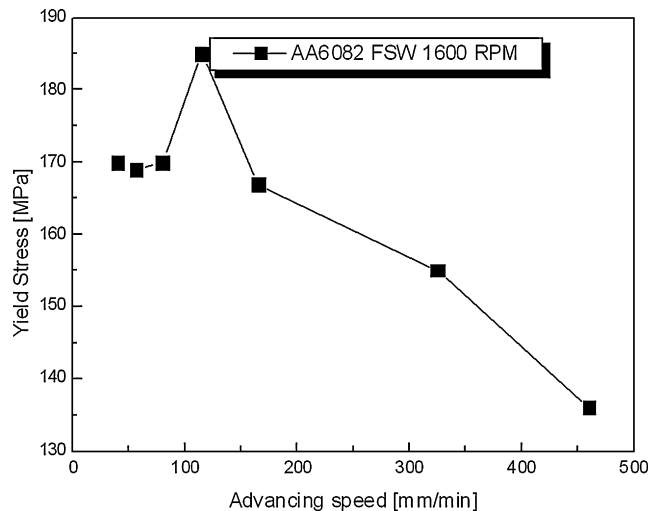


Fig. 10 – Yield stress as a function of welding speed.

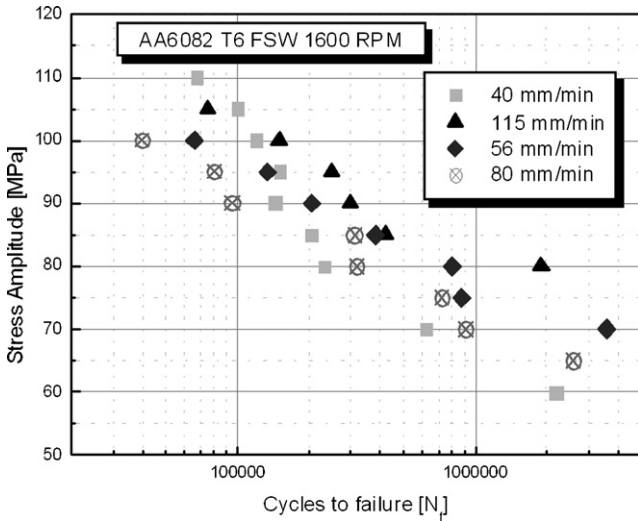


Fig. 11 – Fatigue endurance curves of the studied joints for the following welding speeds: 40, 56, 80 and 115 mm/min.

the force decreases linearly as increasing the revolutionary pitch. In Fig. 7 the authors correlated the coupling effect of force and temperature to the measured grain size in the same zone. From such observation it clearly appears how the most effective recrystallization effect is reached when such ratio has a value close to 70. In fact, other authors observed an increase in the peak temperature as increasing the revolutionary pitch and a strong effect of travel speed (at the same tool rotation speed) on the material mixing; for this reason it was important to couple such parameters to the resultant mean grain size. By decreasing the temperature in the nugget zone the force acting on the material is not able to produce a plastic flow proper of a continuous dynamic recrystallization process, while by increasing the temperature of the material for travel speed too low for the used welding speed the material is extremely softened and can be subjected to grain growth after deformation.

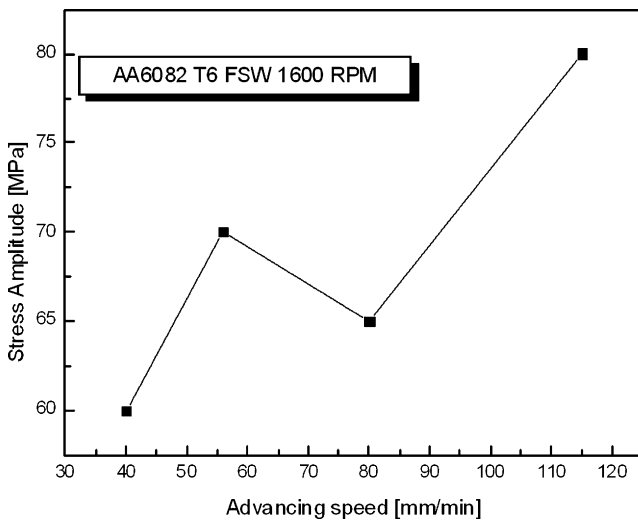


Fig. 12 – Variation of the stress amplitude at 2×10^6 cycles to failure, as a function of welding speed.

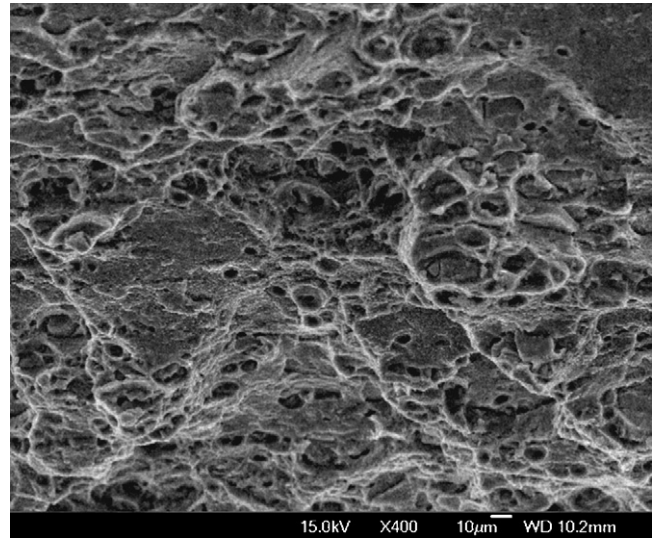


Fig. 13 – Fracture surface of the tensile tested specimen at a welding speed of 115 mm/min.

3.3. Mechanical properties

The base metal tensile properties of heat-treated 6082 aluminium alloy sheets are shown in Fig. 8. For the welded joints, strong ductility variations, calculated as strain to fracture (Fig. 9), and yield strength variations (Fig. 10) were measured as a function of the different advancing speeds. The yield strength increases rapidly from the lower speeds up to 115 mm/min speed; the maximum yield point value is found to be around 185 MPa and then decreases again with highest speeds, revealing strong hardening phenomena to take place over a certain tool advancing speed limit, for which the stirring effect is presumably less efficient and the material originated from the leading edge in one single sheet does not travel enough into the coupled sheet material. On the other hand, the material ductility seems to follow the same behaviour and the optimal mechanical properties with elongation equal to 11.6% are achieved around 115 mm/min tool speed value, after which a sensible ductility reduction appears.

The fatigue properties of the FS welded joints can be observed in S-N curves for the toughest studied joints, as shown in Fig. 11. The fatigue specimens have been cut from the welded plates in a number of 25 for each condition and polished, according to standard procedures and avoiding superficial defects. The bead material in all the welding configurations shows similar fatigue behaviour in the low cycle regime, since extremely narrow data differences are produced in terms of stresses; in the high cycle regime, the Wöhler curves reach clear differences between the joints obtained with different welding speeds, even that a small number of data are available for each condition; this leads to decreasing stress amplitude limits as function of life endurance up to the fatigue limit (2×10^6 cycles to failure) and in dependence of the technological parameters. According to the static tests results, the material welded with the advancing speed of 115 mm/min exhibits optimal fatigue properties and the

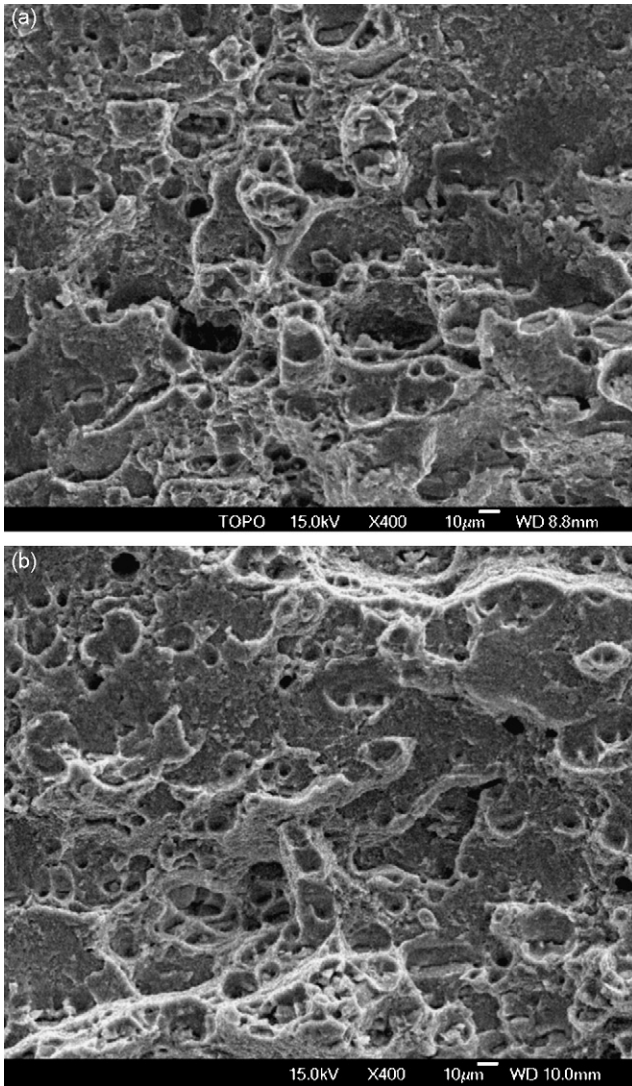


Fig. 14 – Fracture surfaces of the tensile tested specimens at a welding speed of 80 mm/min (a) and 325 mm/min (b).

higher fatigue limit is settled around 80 MPa. By considering the same range of cycles to failure in the higher regime, the stress amplitude variation and the fatigue limit with respect to the advancing speed is shown in Fig. 12; the stress amplitude is confined in a small range and increases strongly with respect to other welding conditions at the advancing speed of 115 mm/min. By considering an uniform FSW welding parameter, the “revolutionary pitch” is conventionally used and defined actually as the advancing speed/rotating speed; from many data available in literature, the optimum FSW conditions are those for which the revolutionary pitch results close to 0.1 (Mishra and Ma, 2005). In the present case both the tensile properties and the fatigue limit of the S–N curves increase from the lower speeds up to different values close to 0.07 and then such properties decrease. This fact is due to the optimal combination between the material plasticization during tool rotation and the mixing affect produced by the advancing movement. The tool advancing action (inclined at a certain angle) is extremely

similar to an extrusion process which requires optimal temperature conditions for the better quality of the material in terms of microstructure (Buffa et al., 2006); consequently, since the resultant fatigue behaviour for butt welded joints is directly related to the microstructure, provided that porosities occurrence is avoided and micro-cracks formation is absent, and considering that stress concentrators are missing, the studied FS welded joints offer the best fatigue performances only when optimal microstructure configurations are reached. With a revolutionary pitch in the range of 0.07–0.1, the process is in the optimal temperature and strain rates conditions to produce good microstructure quality without defects for 6082 FSW butt joints and therefore sound welds are achieved.

3.4. Fractography

The SEM observations of the fracture surfaces of the tensile tested specimens revealed the best bonding characteristics of the joints obtained at 115 mm/min. The fracture surface appears populated of very fine dimples revealing a very ductile behaviour of the material before failure (Fig. 13).

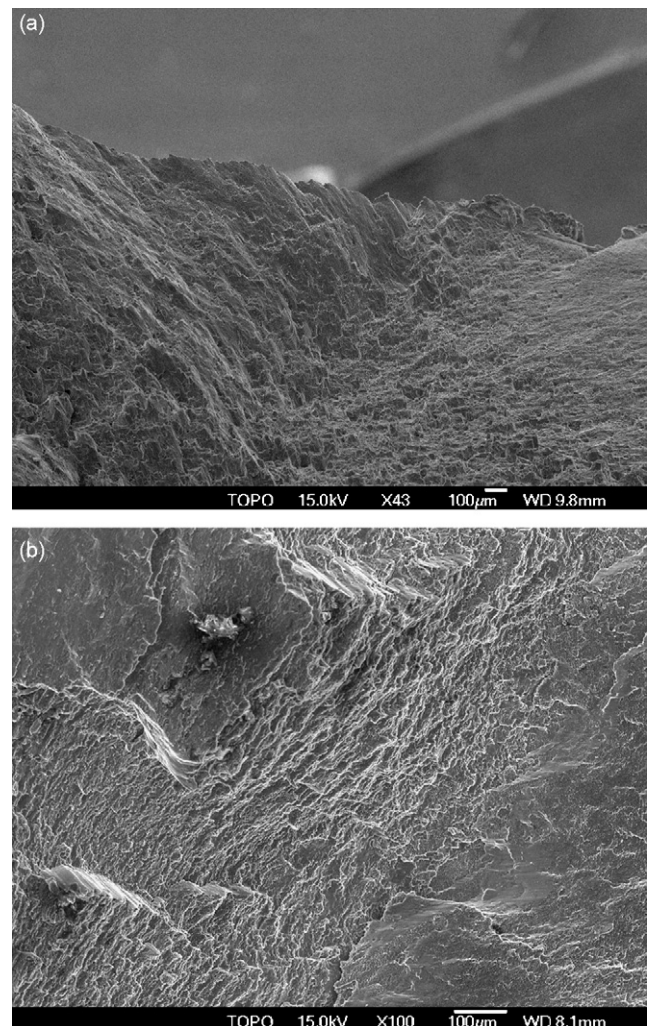


Fig. 15 – Fracture surfaces of the fatigue specimens (welding speed of 115 mm/min) tested at 100 MPa (a) and 95 MPa (b).

On the contrary a less ductile behaviour was revealed by the surfaces of joints produced in different conditions of welding speed; at 80 mm/min (Fig. 14a) and 325 mm/min (Fig. 14b) a minor population of voids larger in size were developed.

All the fatigue tested specimens was observed to fracture in the advancing side of the tool. By observing the fracture surfaces of the fatigue tested specimens welded at 115 mm/min it was observed that, at higher stresses the fatigue cracks started from the surface. In Fig. 15 the fatigue crack and the fast region of the specimens failed at 100 and 95 MPa stress amplitude is shown; such big defects are often associated with the vortex formed in the material in the advancing side where a more chaotic flow is formed leading to the presence of voids of the mean dimension of hundreds of microns that represent the site of fatigue cracks initiation. By decreasing the stress amplitude a strong change in the crack behaviour was detected, the cracks appear to start from the forging defects inside the joints which are always present in this kind of weldings (Fig. 16). The failure is also related to the coalescence of many small voids and defects in the material (Fig. 17). The presence of dimples on the surface revealed a local ductile

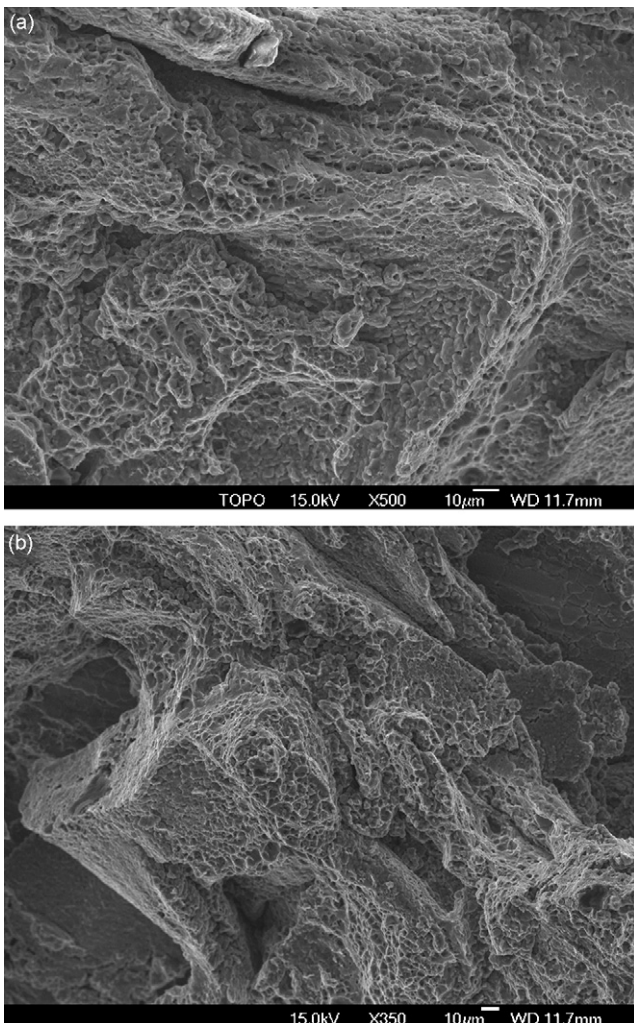


Fig. 16 – Fracture surfaces of the fatigue specimens (welding speed of 115 mm/min) tested at 85 MPa (a) and 80 MPa (b).

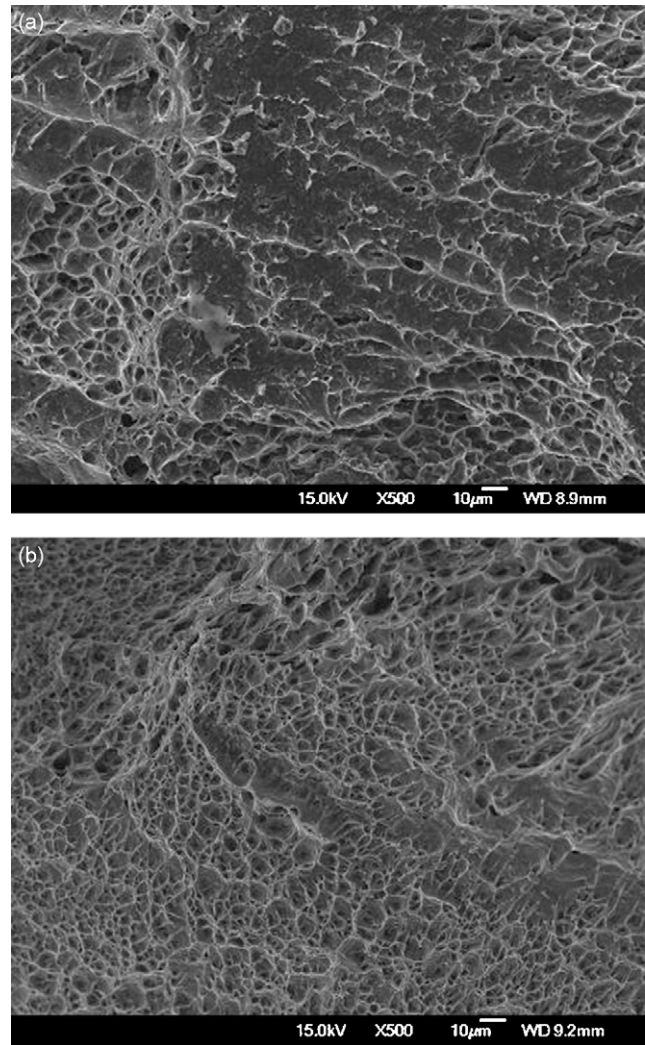


Fig. 17 – Fracture surfaces of the fatigue specimen (welding speed of 115 mm/min) tested at 70 MPa.

behaviour of the material prior to fracture. Such behaviour was observed on the whole fracture surface revealing the observations previously explained on the optimal deformation conditions (temperature and strain rate) necessary to obtain good quality material after deformation. This is the case of such conditions in which the optimal solution between material mixing and grain refinement is obtained (Fig. 5). By increasing the advancing speed of the tool and then the revolutionary pitch the material is extruded too fast (high strain rates) and then they are not reached the conditions for the optimal mixing. In the case of an advancing speed of 56 mm/min the fracture surface can be observed in Fig. 18. In such case the big flow line of low plasticized material are evident in a several way. Such irregular flow zones represent the preferential site for crack initiation leading to the final failure. On the other hand, by increasing the revolutionary pitch different fracture mechanisms can be observed. In Fig. 19 it is shown the fracture surface of a specimen welded by employing an advancing speed of 325 mm/min. In this case the main fracture mechanism results the cleavage accompanied with

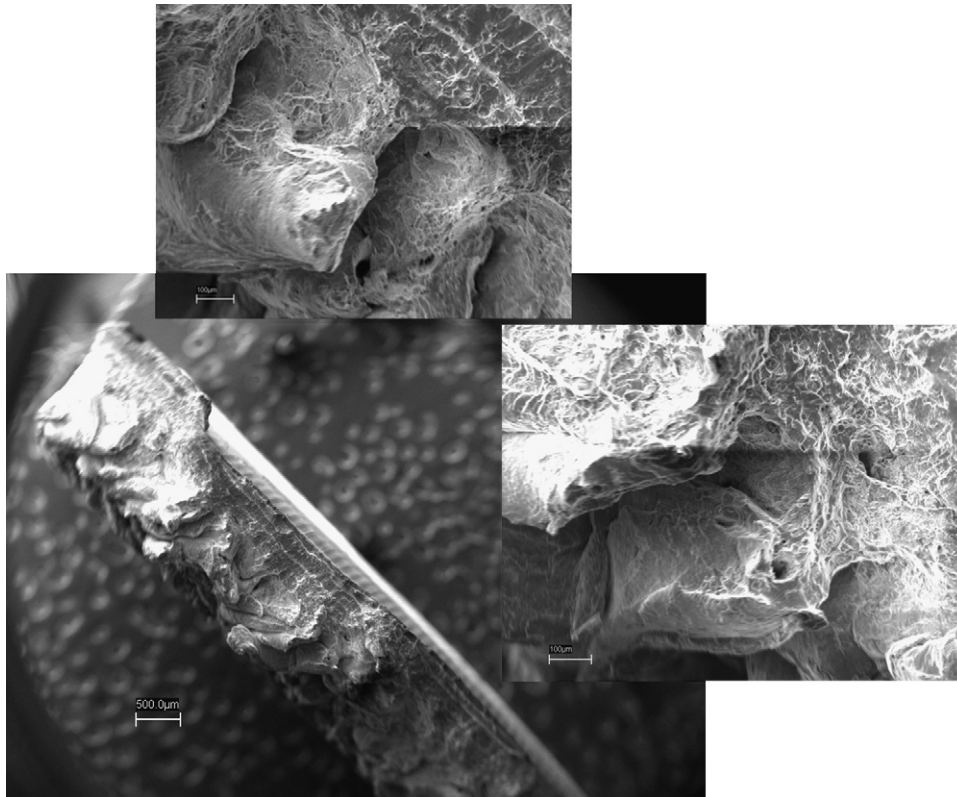


Fig. 18 – Fracture surfaces of the fatigue specimen (welding speed of 56 mm/min) tested at 80 MPa.

small specimen zones of local ductility aspect (dimples). This aspect has been attributed to the heating of the material during welding. The coupling of a high rotation speed and an high advancing speed leads to a good material mixing but to a non

optimal grain structure. The too high strain rate, acting on the material during deformation, causes a boundary weakening of the recrystallized structure which can be visualized by cleavage fracture.

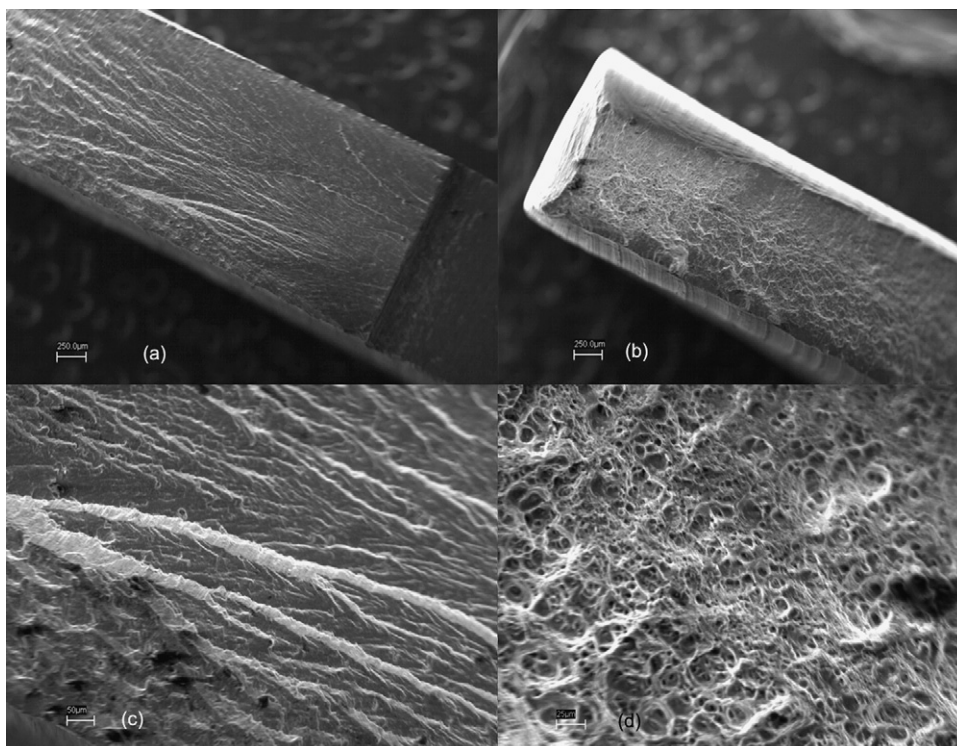


Fig. 19 – Fracture surfaces of the fatigue specimen (welding speed of 325 mm/min) tested at 80 MPa.

4. Conclusions

The effect of welding speed (with advancing speed in the range 40–460 mm/min) on the mechanical and microstructural properties of AA6082 were studied in the present paper. A strong variation in the nugget mean grain size was observed by increasing the advancing speed from 40 to 165 mm/min up to a plateau corresponding to no further variations by increasing the speed up to 460 mm/min. The yield strength was recorded to increase strongly from the lower speeds to 115 mm/min and after starts to decrease by increasing the advancing speed, the ductility of the material followed the same behaviour but restarted to increase after 165 mm/min. The material welded with the advancing speed of 115 mm/min exhibited the best fatigue properties and the higher fatigue limit, while a very narrow similar behaviour in the low cycle regime, differing strongly by decreasing the stress amplitude up to the fatigue limit, was observed in all the configurations. The SEM observations of the fatigue specimens, welded at 115 mm/min, showed that at higher stress amplitude levels the cracks initiate at the surface of the welds. By decreasing the stress amplitude the cracks initiate by the internal defects.

REFERENCES

- Berbon, P.B., Bingel, W.H., Mishra, R.S., Bampton, C.C., Mahoney, M.W., 2001. Friction stir processing: a tool to homogenize nanocomposites aluminum alloys. *Scripta Mater.* 44, 61–66.
- Buffa, G., Donati, L., Fratini, L., Tomesani, L., 2006. Solid state bonding in extrusion and FSW: process mechanics and analogies. *J. Mater. Process. Technol.* 177, 344–347, Issues.
- Bussu, G., Irving, P.E., 2003. The role of residual stress and heat affected zone properties on fatigue crack propagation in friction stir welded 2024-T351 aluminium joints. *Int. J. Fatigue* 25, 77–88.
- Cavaliere, P., Squillace, A., Campanile, G., Panella, F., 2006. Effect of welding parameters on mechanical and microstructural properties of AA6056 joints produced by friction stir welding. *J. Mater. Process. Technol.* 180, 263–270.
- Dickerson, T.L., Przydatek, J., 2003. Fatigue of friction stir welds in aluminium alloys that contain root flaws. *Int. J. Fatigue* 25, 1399–1409.
- Ericsson, M., Sandstrom, R., 2003. Influence of welding speed on the fatigue of friction stir welds, and comparison with MIG and TIG. *Int. J. Fatigue* 25, 1379–1387.
- Guerra, M., Schmidt, C., McClure, J.C., Murr, L.E., Nunes, A.C., 2003. Flow patterns during friction stir welding. *Mater. Character.* 49, 95–101.
- Hassan, A.A., Prangnell, P.B., Norman, A.F., Price, D.A., Williams, S.W., 2003. Effect of welding parameters on nugget zone microstructure and properties in high strength aluminium alloy friction stir welds. *Sci. Technol. Weld. Join.* 8, 257–268.
- James, M.N., Bradley, G.R., Lombard, H., Hattingh, D.G., 2005. The relationship between process mechanisms and crack paths in friction stir welded 5083-H321 and 5383-H321 aluminium alloys. *Fatigue Fract. Eng. Mater. Struct.* 28, 245–256.
- Jata, K.V., Sankaran, K.K., Ruschau, J., 2000. Friction-stir welding effects on microstructure and fatigue of aluminum alloy 7050-T7451. *Metall. Mater. Trans.* 31A, 2181–2192.
- John, R., Jata, K.V., Sadananda, K., 2003. Residual stress effects on near threshold fatigue crack growth in friction stir welded aerospace alloys. *Int. J. Fatigue* 25, 939–948.
- Lockwood, W.D., Tomaz, B., Reynolds, A.P., 2002. Mechanical response of friction stir welded AA2024: experiment and modelling. *Mater. Sci. Eng. A* 323, 348–353.
- Mishra, R.S., Ma, Z.Y., 2005. Friction stir welding and processing. *Mater. Sci. Eng. R* 50, 1–78.
- Rhodes, C.G., Mahoney, M.W., Bingel, W.H., 1997. Effects of friction stir welding on microstructure of 7075 aluminium. *Scripta Mater.* 36, 69–75.
- Sato, Y.S., Urata, M., Kokawa, H., Ikeda, K., 2003. Hall-/Petch relationship in friction stir welds of equal channel angular-pressed aluminium alloys. *Mater. Sci. Eng. A* 354, 298–305.
- Ulysse, P., 2002. Three-dimensional modeling of the friction stir-welding process. *Int. J. Mach. Tools Manuf.* 42, 1549–1557.